A MULTI-STATISTICAL ANALYSIS OF THE SOUTHERN OSCILLATION (SO) AND ITS RELATION TO THE MEAN MONTHLY ATMOSPHERIC CIRCULATION AT 500 hPa IN THE NORTHERN HEMISPHERE

Shi Neng (施 能)

Nanjing Institute of Meteorology, Nanjing

Received July 2, 198

ABSTRACT

In this paper the correlation analysis, factor analysis, fuzzy classification, and principal component analysis (PCA) are performed for the southern oscillation index (SOI) from the Climate Analysis Center (CAC) at the NOAA. It is shown that the 12-month SOI can be classified into two groups: one from January through April and the other from May through December. They differ in persistency and correlation. It is also found that the year of strong or weak SO can be defined by the first principal component of the SOI. The 11 years of weak SO thus defined contain 9 El Nino events.

In addition, the relations between the SOI and 500 hPa geopotential height, mean monthly zonal height, mean monthly interzonal height differences, centers of atmospheric activities, characteristics of the atmospheric circulation (the intensity index of the north polar vortex, the area index of the subtropical West Pacific high, mean monthly zonal and meridional circulation indexes in Asia and Eurasia) in the period of 24 months from January through December of the next year have been examined on the basis of the monthly data from 1951 through 1984. The correlation coefficients and Mahalanobis distances are thus presented. Analysis indicates that in the early part of the low SOI year, i.e., in April, the 500 hPa geopotential height north of 75°N is significantly low and then becomes higher in May. It is found that in April the trough of the first harmonic wave is in the Eastern Hemisphere and the contribution of its variance is smaller than in May. Analysis shows that the opposite is true in the high SOI year. Such variation in the height field during the April–May period is an early signal of the SO at higher latitudes.

In the end, a statistical prediction model for the SOI is presented, by means of which a low SOI year as well as an El Nino event has been successfully predicted for 1986.

1. INTRODUCTION

The southern oscillation (SO), discovered by Walker (1924), is a large-scale fluctuation of the atmospheric circulation representing a tendency of the equatorial Indian Ocean pressure to be above (or below) normal when the tropical South Pacific Ocean pressure is below (or above) normal. Bjerknes (1969) and Quinn (1974) pointed out that this fluctuation in the surface pressure was related to the sea surface temperature (SST) in the equatorial East Pacific, particularly, to the abnormal warming of the SST off the coast of Peru known as El Nino. Great interest was thus arisen once again among the meteorologists. Chen (1982) and Trenberth (1983) assessed the index representing the intensity of the SO, i.e., the southern oscillation index (SOI). However, the statistical characteristics, persistency and correlation of the seasonal and monthly SOI values have not yet been discussed. Chen (1982) used the seasonal means of the SOI, obtained by averaging

the three adjacent monthly values centered in January, April, July and October respectively, as the index representing the SO intensity. And van Loon and Repapis (1982) used not only the pressure at sea level but also the rainfall at the equatorial stations in the Pacific when he selected the SO extreme values. A link of the SO to the mid-latitude weather systems has been observed by Bjerknes (1969) and most recently by Chen (1982), van Loon and Repapis (1982) and Rogers (1981), and van Loon and Maddgen (1981). However, most of the work done has been limited to the low and middle latitudes in the winter months (December, January and February) and the relations between the SO and the 500 hPa height field at higher latitudes have not been discussed in detail.

In this paper, an index representing the abnormal year of the SO is presented and the years of the SO extreme values are selected on the basis of the statistical analysis of the SOI from the CAC in the U.S. Then a statistical study is made of the 500 hPa atmospheric circulation of the oscillation extreme values in the 24 months from the current year to the following year so as to improve our understanding of the effect of the oscillation on the zonal circulation in different months and regions.

II. MULTI-STATISTICAL ANALYSIS OF THE SOI

In order to make better use of the SOI, multi-statistical analysis is necessary. The main data used in this analysis are those of the SOI from the CAC in the U.S. during the 1935–1985 period.

1. *Correlation and Persistency*

By using the data covering 51 years, the correlation matrix ${}_mR_m=(r_{ij})$, $m=12$ can be calculated. It is apparent from the value of r_{ij} that the correlation coefficients fluctuate between 0.494 and 0.814 from June to December and between 0.142 and 0.592 from January to May. In contrast, the correlation coefficients of the SOI between January to May and June to December fluctuate between -0.187 and 0.558. This shows that the monthly data of the SOI from January to May differ greatly from those from June to December. It is found by calculating $R_i=\frac{1}{11}\sum_{j=1,\,j\neq i}^{m}|r_{ij}|$ that the months of the maximum R_i in the four seasons will be April, August, October and December respectively. Thus these months can be used as the typical months in the corresponding seasons. This conclusion is in good agreement with the conclusion arrived at by using the principal component analysis. The maximum of R_i is R_s and the minimum is R_t for all the 12 months in a year.

Figure 1 gives the one-to-twelve-month lag correlation coefficients. It is apparent from the isopleth of the correlation with 5% significance ($|r|=0.28$) that the time of persistency correlation from January to April is the shortest and decreases with month, i.e., from three months for January to one month for April. This means that the correlation coefficients of the SOI between January–April and May are very small. However, after May the lag correlation month with 5% significance suddenly increases to nine months and lasts until August. Then it begins to decrease linearly until December when the number of the lag month is only four. Such persistency makes all the beginning months of the lag correlation with 5% significance last until April of the following year. This

means that April is the most abnormal month of the SOI.

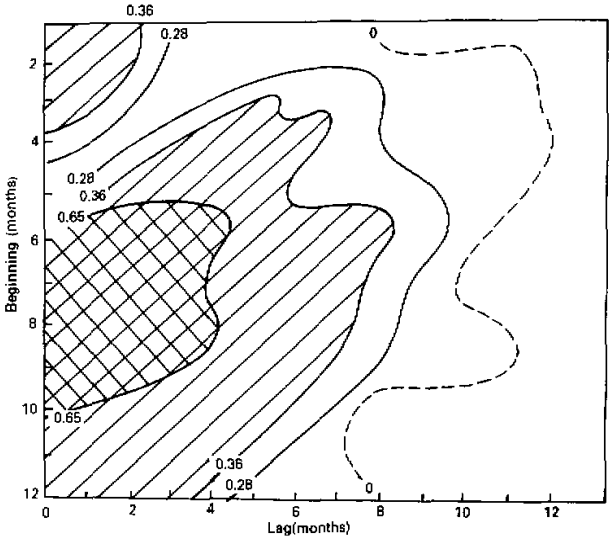

Fig. 1. Lag correlation coefficients of the SOI.

2. *Factor Analysis of the SOI*

By factor analysis we have calculated the eigenvalues and eigenvectors of the matrix ${}_mR_m$ and thus find the factor loading matrix $A=(a_{ij})$

$$a_{ij}=\sqrt{\lambda_i}V_{ij} \qquad i,j=1,2,\cdots,12,$$

where V_{ij} is the i-th component of the j-th eigenvector in the matrix ${}_mR_m$, a_{ij} is the correlation coefficient between the value of the i-th month of the SOI and the j-th principal component of the SOI. λ_i is the eigenvalue (see Table 1). It is shown from Table 1 that the first two eigenvectors can provide 67.85% of the SOI information of 12 months, and thus the factor loading diagram with two factors is given in Fig. 2.

Table 1. Eigenvalues of the SOI and Its Accumulative Rate

j	1	2	3	4	5	6	7
λ_j	5.78	2.36	0.79	0.59	0.51	0.45	0.40
$\left(\sum_{i=1}^{j}\lambda_i/12\right)\times 100\%$	48.15	67.85	74.74	79.42	83.66	87.41	90.76

It is apparent from Fig. 2 that the 12-month SOI values can be classified into two groups.

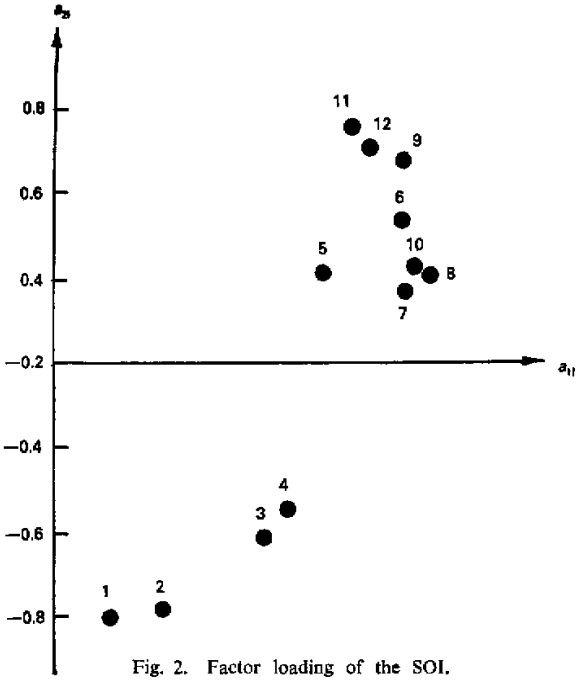

Fig. 2. Factor loading of the SOI.

3. *Fuzzy Classification Analysis*

By fuzzy classification, the 12-month SOI values are classified. The result at various analogy levels λ is given in Fig. 3.

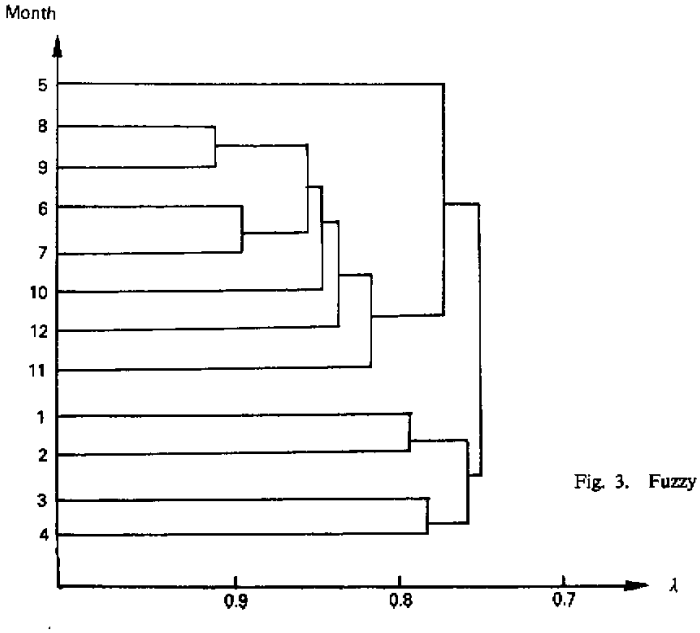

Fig. 3. Fuzzy classification of the SOI.

It is found from Fig. 3 that if we divide the 12-month SOI's into two groups, we have one from January through April and the other from May through December and if we divide them into three groups, we have one from January through April, one in May and one from June through December. This agrees with the conclusion arrived at by factor analysis.

4. *Principal Component Analysis (PCA)*

Table 1 shows the eigenvalues of the SOI by PCA. The first eigenvector is V_1 (which has been multified by 10). V_1=(0.49 1.09 2.05 2.28 2.68 3.48 3.50 3.71 3.51 3.57 2.93 3.19). It is seen that the weight is the greatest in August and the smallest in January. Fig. 4 shows the annual values of the first principal component of the SOI. The symbol E means the El Nino year (denoted by EN in the following discussion). It is noted that low-value years of the first principal component are almost exclusively EN years and vice versa. By calculation the correlation coefficient between the first principal component and the annual mean value of the SOI is 0.90. However, as the former has a maximum variance and is more correlated with the EN year than the annual mean value, it can be used as the index of the anomaly of the SO year.

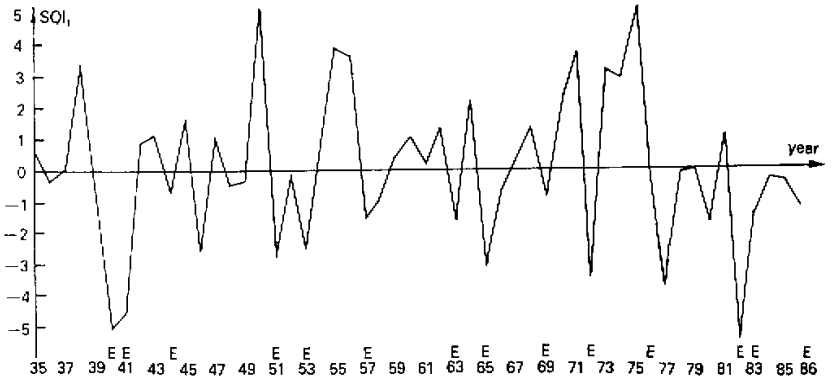

Fig. 4. The first principal component of the SOI.

III. REGIONS AND MONTHS IN WHICH THE SO HAS A SIGNIFICANT EFFECT ON THE ATMOSPHERIC CIRCULATION

Most of the past study was restricted to the circulation in the winter months (December, January and February). In order to find the precursors of the SO and improve forecasting intervals, it is necessary to increase the time range in this study to 24 months, i.e., all the 24 months in the current and following years, and then test the results statistically.

1. *Extremes of the SO*

It is seen from the above-mentioned that the first principal component of the SOI can represent the annual anomaly of the SO. In practice, it is an unequal weighted mean of

the monthly value of the SOI and is more reasonable than the annual mean value of the SOI. For this reason, a year with the value of the first principal component of the SOI −1.0 or less is defined as the low value year of the SO (denoted by SL) and a year with the value 2.0 or more as a high value year of the SO (denoted by SH). An examination of the series of the first principal components reveals that years of SL are 1951, 1953, 1957, 1963, 1965, 1969, 1972, 1977, 1980 1982 and 1983, of which there are 9 El Nino years, and that years of SH are 1955, 1956, 1964, 1971, 1973 1974 and 1975, which have been cited as anti-El Nino years by some authors.

2. *Methods and Result from Computation*

First, computation is made of Mahalanobis distance $(Maha)_{it}$ for the SL and SH in the current and following years at the grid of 10° latitude 5° longitude from 10°N to 85°N in the 500 hPa height field. Mahalanobis distance is the space distance in a broad sense, similar to "t" statistics. It is found that the greater the value of $(Maha)_{it}$ is, the more significant the difference is between the SL and SH years at the i-th point in the t-th month.

$$(Maha)_{it}=(H_i/\sigma_i)_t^2 \quad t=\overline{1,24}, \quad i=\overline{1,576}$$

where H_i is the difference of the monthly mean height at the i-th point between the SL and SH years, and σ_i is the standard deviation of the height field at the i-th point.

Table 2 shows the monthly value of $(Maha)_{it}$ with certain significance. It is seen that in the Northern Hemispheric 500 hPa height field the statistically significant difference, which has been shown in April of the current year, increases to a maximum in February of the following year, and lasts until early autumn.

Table 2. The Number of $(Maha)_i$ with Certain Significance

Significance \ Month	1	2	3	4	5	6	7	8	9	10	11	12
0.05	44	19	25	87	114	70	40	57	56	109	71	71
0.01	1	1	6	27	57	20	10	24	15	58	37	43
0.001	0	0	0	3	18	6	1	7	8	16	20	15
Significance \ Month	1	2	3	4	5	6	7	8	9	10	11	12
0.05	115	163	83	88	89	45	32	54	51	19	8	10
0.01	68	94	49	40	33	17	3	5	12	0	1	0
0.001	33	38	14	11	7	7	0	1	1	0	0	0

Table 3 is the distribution of the points with 0.05 significance in different months and latitudes. It is seen that the number of the points varies with month and latitude. Points south of 30°N account for 56% of the total. The total number in the current

year is significantly larger than that in the following year north of 60°N. However, the opposite is true south of 35°N.

Table 3. The Number of the Points of $(Maha)_i$ with 0.05 Significance

Latitudes		85	80	75	70	65	60	55	50	45	40	35	30	25	20	15	10
In the current year	1	14	9	7	5				1	4	2					1	1
	2		3	4	2					1	2	4	1				2
	3					2	4	5	4		3	3					4
	4	19	14	9	4	6	4					2	3		1	8	17
	5	36	35	11	3	3	3	2						1	1	6	14
	6				1	1	2	3	3	3	1	1	3	3	10	16	23
	7					2	1	1	1		2	2	6	4	11	5	5
	8							2		2	2	5	3	10	10	10	13
	9					1				2		4	1	4	8	15	22
	10	12	9	8	9	7	7	2	1	4	3	2	5	4	8	12	16
	11						1	3	6	8	6	1	1	5	10	12	17
	12					1	1						2	3	8	25	31
In the following year	1		4				2	4	2	3	2		3	9	20	30	36
	2					6	11	17	14	5	5	6	6	9	19	31	34
	3								2				2	7	12	28	32
	4		6				1	1	2			2	4	7	10	25	30
	5					1		2	3	2		7	10	11	17	19	17
	6						1				1	6	8	8	16	8	7
	7					2	1		1	2	5	3	7	2		5	4
	8		6	3		4	4	1	3	2	4	5	5	7	5	3	2
	9			1	2	3	2	3	6	7	3	5	7	2	2	4	4
	10			4	6	3					2	2	1	1			
	11									1		2	1	1			2
	12	10															
The total in the current year		81	71	39	24	23	23	18	16	24	21	24	25	33	67	110	165
The total in the following year		10	16	9	8	19	22	28	33	22	22	38	54	64	91	153	168

IV. CHARACTERISTICS OF THE 500 hPa CIRCULATION DURING THE YEAR OF THE SO

1. *At High Latitudes (North of 75°N)*

It is shown from Table 3 that the circulation in January, April, May and December varies between the SL and SH years. The components of the height field (omitted) show that the geopotential height in January of the SL year increases significantly, for example, by 80–100 geopotential meters north of Alaska and in April decreases, especially north of Tamil I. by 50–70 geopotential meters on the average. In May it increases again and the increment is three times the standard deviation north of Greenland. As the circulation at low and middle latitudes varies only slightly during April and May, the variation of the height field at high latitudes can be taken as an early signal of the SO at these latitudes.

The first row in Table 4 shows the correlation between the geopotential height at the center of the North Polar vortex, i.e., the intensity index of the North Polar vortex, and the first principal component of the SOI. Values smaller than 0.18 are only indicated by the positive or negative signs in the table. It is seen that the intensity index of the North Polar vortex can also show the characteristics mentioned above but is not so clear as the height field. And the month-wise test of the Mahalanobis distance of the intensity index of the North Polar vortex shows that the difference is significant in May, reaching 0.05 significance (the value amounts to one standard deviation).

Table 4. The Correlation of the First Principal Component of the SOI to the Intensity Index of the North Polar Vortex and the Area Index of the Subtropical West Pacific High

Months	1	2	3	4	5	6	7	8	9	10	11	12
The intensity index of the North Polar vortex	−0.25	—	+	0.18	−0.19	—	—	0.24	—	—	−0.32	—
The area index of the subtropical West Pacific high	—	—	—	—	—	—	−0.19	−0.24	−0.26	−0.32	−0.63	−0.65
Months	1	2	3	4	5	6	7	8	9	10	11	12
The intensity index of the North Polar vortex	+	+	+	+	0.21	0.26	—	—	—	—	—	—
The area index of the subtropical West Pacific high	−0.72	−0.79	−0.57	−0.47	−0.40	−0.52	−0.24	−0.31	−0.43	−0.18	+	+

Tables 5 and 6 show the positions and variance contributions of the first and second harmonic waves. For the sake of simplicity, Table 4 only gives the significant months and the positions of the first trough, and the positions of the second trough can be determined by adding 180 degrees longitude.

Table 5. Positions of the First and Second Troughs in the SL Year (the first row) and SH Year (the second row). 85°N.

Months	*1*	*3*	*4*	*7*	*10*	*1*	*3*	*6*	*7*	*8*	*9*	*11*
The first wave	19°W	39°W	91°E	83°W	119°W	52°E	45°W	65°E	103°W	61°W	82°W	33°W
	161°W	57°W	92°W	113°W	125°E	95°W	73°W	87°W	121°W	152°W	165°W	130°W
The second wave	94°E	101°E	101°E	87°E	108°E	99°E	95°E	117°E	152°E	83°E	87°E	109°E
	91°E	74°E	74°E	118°E	104°E	100°E	110°E	101°E	114°E	130°E	107°E	107°E

It is shown from Table 5 that in April and in January and June of the following year the first trough is located in the Eastern Hemisphere for the SL year and in the Western Hemisphere for the SH year, and in October the trough is located in the Western Hemisphere for the SH year and in the Eastern Hemisphere for the SL year and that the second trough is found to shift 27° longitude further east in April, 31° longitude further west in

July, 15° longitude further west in May of the following year, 38° longitude further east in the June–July period and 47° longitude further west in August for the SL year than for the SH year.

It is shown from Table 6 that the variance contribution of the first wave in January and May of the SL (SH) year and in May of the following SL (SH) year is greater (smaller) than that of the second wave. The minimum variance contribution of the first wave in April is an early signal of the SL year at higher latitudes. And from June to next March the variance contribution of the second wave in the SL year is always greater by 20% on the average than that in the SH year.

Table 6. The Variance Contribution of the First and Second Waves in the Extreme Year and the Following Year of the SO at 85°N. (The first wave/The second wave)

Months		1	2	3	4	5	6
In the current year	SL	61.8/36.7	54.7/43.6	77.0/22.4	4.4/90.7	60.3/34.3	43.1/40.8
	SH	29.1/63.7	97.2/1.8	58.8/38.0	92.8/5.7	37.5/60.8	83.6/14.4
In the following year	SL	83.0/34.9	73.2/26.0	70.7/28.7	77.3/21.9	85.5/13.2	90.0/5.2
	SH	83.9/14.6	89.5/8.3	89.6/8.4	70.3/25.0	9.7/77.6	85.5/11.2
Months		7	8	9	10	11	12
In the current year	SL	82.9/11.2	96.0/2.2	65.5/32.8	83.7/13.6	67.8/29.0	69.6/30.0
	SH	98.8/0.1	86.7/1.0	94.7/3.7	93.8/5.0	92.8/2.5	94.6/4.8
In the following year	SL	91.6/6.0	83.8/13.8	80.4/15.6	83.1/15.0	73.1/25.2	57.7/39.3
	SH	92.4/3.0	89.3/5.3	56.9/40.7	88.6/11.0	97.6/1.6	75.5/23.5

2. *At Low Latitudes (South of 30°N)*

Fig. 5 shows the time section at 500 hPa along 15°N. It is seen that the low-latitude circulation varies during the period from spring to the autumn of the following year. Besides, there is a high at the 5880 geopotential height at 120°E–180°E from September to next July in the SL year but no high is found in the SH year, and there is a low at the 5840 geopotential height at 170°E–110°W from November to next April and at 30°W–70°E from November to next February in the SH year but no low is found in the SL year.

As shown in Table 4, almost all the correlation coefficients between the SOI and the area index of the subtropical West Pacific high are negative. The maximum negative value (−0.792) occurs in February of the following year.

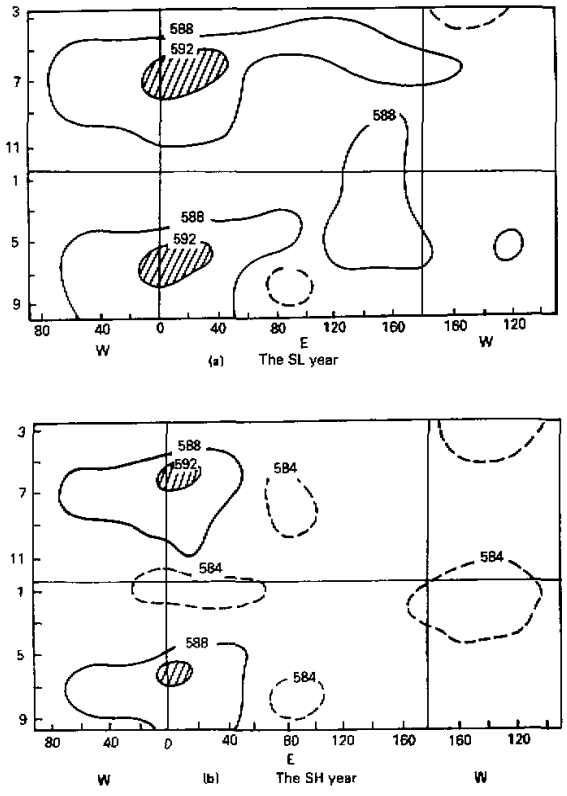

Fig. 5. Time section at 500 hPa along 15°N.

3. *At Middle Latitudes* (35°*N*–65°*N*)

Significant difference in the circulation is found near North America, Aleutians, Iceland and Alaska. Fig. 6 shows the anomalies at the 500 hPa geopotential height in the area of Aleutian (7 grid points, 55°N, 175°E–170°W, 45°N, 170°E–175°W, 50°N and 170°E–170°W) and in the area of Iceland (7 grid points, 65°N, 35°W–15°W, 60°N, 30°W–10°W, 65°N and 15°W).

It is shown from Fig.6 that the height in the Aleutian area is apparently positive anomalous in January of the SH year and from September on the difference between the SH and SL years becomes gradually significant, i. e., the Aleutian low becomes deepened and reaches a minimum next February. The height in the area of Iceland is positive anomalous in March and October of the SH year and negative anomalous in October of the SL year, and after that time the value becomes comparatively low. Then in next January the Iceland low becomes deepened in both the SL and the SH years and is more intense in the SH year than in the SL year.

The North American high has the maximum positive anomaly in February of the following year.

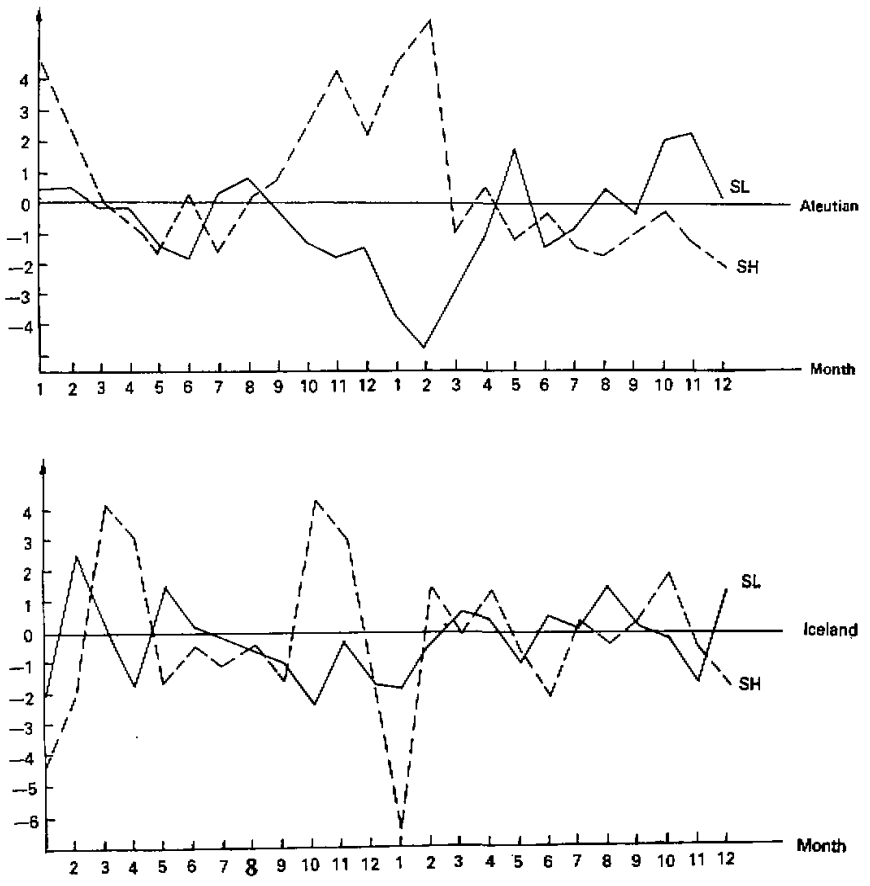

Fig. 6. Anomalies at the 500 hPa geopotential height in the area of Aleutian and Iceland.

V. THE RELATIONSHIP BETWEEN THE SO AND THE MEAN MONTHLY ZONAL HEIGHT

Fig. 7 shows the correlation coefficients between the first principal component and the 500 hPa mean monthly zonal height. It is found that:

1. The correlation area with 0.05 significance ($|r|>0.34$) spreads northward regularly, reaching its northmost position (40°N) in June of the following year. This means that at this time the mean monthly height in the SL year increases significantly. The maximum increment is found at 15°N in January-February of the following year.

2. The mean monthly height at middle and high latitudes decreases from September to next January in the SL year.

3. In the area north of 75°N there is a negative center with 0.05 significance in January and May and a positive center in April, which is in agreement with the result mentioned above.

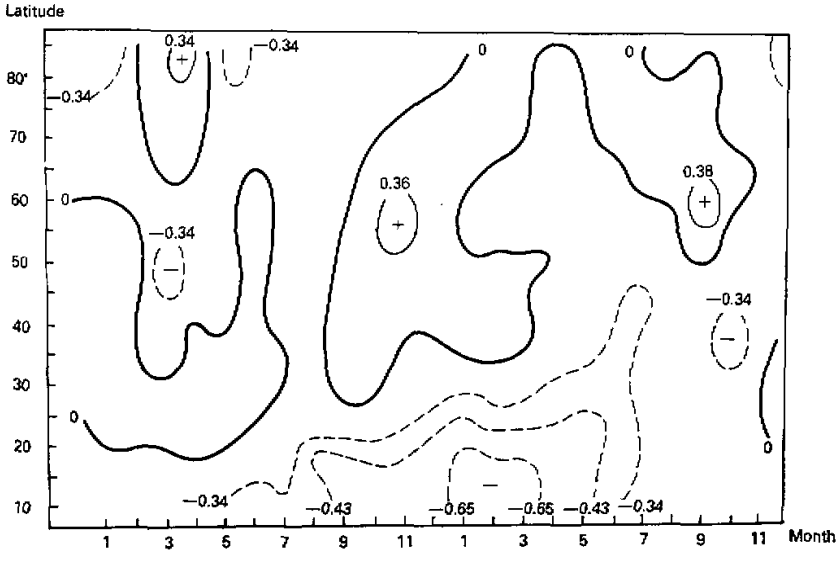

Fig. 7. Correlation coefficients between the first principal component and the 500 hPa mean monthly zonal height.

VI. RELATIONSHIP BETWEEN THE SO AND THE DIFFERENCE IN THE MEAN MONTHLY INTERZONAL HEIGHT

Loon (1981) compared four weak SO years with three strong SO years and obtained: the geostrophic wind tended to intensify south of 45°N and to weaken north of 45°N during the weak SO year. But his discussion was confined to winter (December, January and February) situations. For simplicity, the mean interzonal height difference (low latitude minus high latitude) is calculated for the SL and SH years, respectively, and thus we have Fig. 8 by subtracting the difference of the SH year from the difference of the SL year. It is found that the basic characteristics of the SL year are:

1. The west flow tends to intensify south of 45°N in January–June but from next January on it becomes weaker south of 15°N and gradually spreads northward to 55°N.

2. The west flow does not consistently weaken north of 45°N. The strength of the west flow varies on the main alternately at high latitudes, and particularly in April-May assumes a strong-to-weak pattern. This coincides with the early signal mentioned above. At middle latitudes the weak west flow prevails north of 45°N but there is an area with an intensified west flow located at 45°N–60°N in June and then in August spreads northward, reaching 70°N–80°N. In autumn, the area with the intensified west flow extends northward to 60°N and the area of the weakened west flow extends up to the North Pole with increased intensity.

3. The west wind becomes weaker at middle latitudes and stronger at high and low latitudes from December to next February and its intensity varies most significantly.

In addition, we have calculated the correlation coefficients between the first principal component and the mean monthly zonal and meridional circulation indices in Asia (60°E–

150°E) and Eurasia (0°–150°E). The result indicates that the negative correlation coefficient with meridional circulation index reaches 0.01 significance in August and September, i. e., the meridional circulation is significantly strong in August and September of the SL year. However, all of the correlation coefficients mentioned above do not reach 0.05 significance.

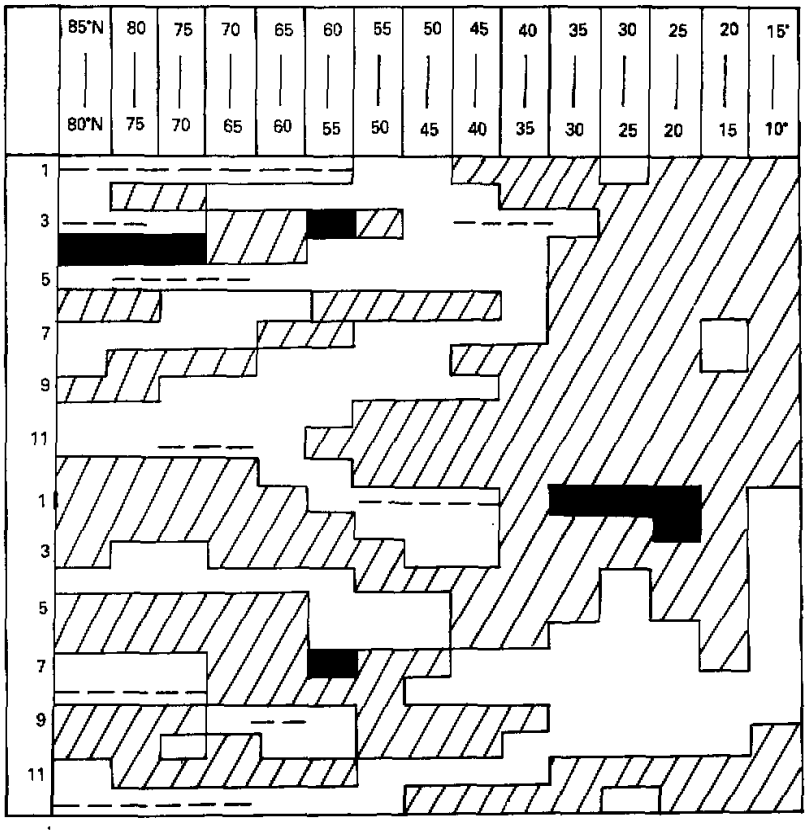

Fig. 8. The 500 hPa interzonal mean monthly height difference in the low SO year minus the 500 hPa interzonal mean monthly height difference in the high SO year (unit: geopotential meters).
Black area: weakened
Dashed line: significantly weakened
Shaded area: significantly intensified
Oblique line: intensified

VII. STATISTICAL PREDICTION OF THE EXTREME YEAR OF THE SO AND EL NINO EVENT

As mentioned above, 9/11 of the SL years defined in this paper are El Nino years and the SH year can be regarded as the anti-El Nino year. However, only when the information on the SOI for all the twelve months is available can the year be defined as the extreme year of the SO. How to predict as early as possible an El Nino year is an interesting question. In this paper stepwise regression is used to select three predictors out of eight

and an equation is established for predicting the first principal component of the SO.

$$Y = 108.98 + 0.188x_1 - 0.118x_2 - 1.249x_3,$$

where

x_1: 500 hPa mean height at 85°N, 10°E–160°E in April,

x_2: 500 hPa mean height at 36 grid points at 85°N in May,

x_3: 500 hPa mean height at 10°N, 10°E–180°E–170°W in May.

The multi-correlation coefficient of the equation is 0.66, the accuracy is 77% when qualitatively diagnosed and the Hedike skill score is 0.66 as compared with the random prediction.

During the April–May period of 1986, a typical early signal for the low SO year appeared. Substituting the independent sample data for the prediction equation yields $y = -1.1$, a low-value year and also an El Nino year; the prediction proves to be perfectly correct.

As the correlation between the monthly value of the SOI before May and that after May is poor, it is difficult to diagnose the extreme year of the SO prior to May. This study is only a try. In diagnosing El Nino, it seems at present necessary to pay attention to some other variations in the circulation besides considering tropical dynamics and use the statistical method.

VIII. SUMMARY AND CONCLUSION

1. The 12-month SOI can be classified into two groups: one from January through April and the other from May through December. The correlation and persistency of the SOI from January through April is poor. April is the month of the most anomalous SOI.

2. The intensity of the SO year can be defined by the first component of the SOI.

3. In the low SOI year, the 500 hPa height north of 75°N is significantly low in April and then increases in May. The trough of the first wave is located in the Eastern Hemisphere in April and in January and June of the following year and in the Western Hemisphere in October. The variance contribution of the first wave is significantly small (less than 10%). The opposite is true in the high SOI year as mentioned above.

4. In fact, the effect of the SO on the circulation during the winter months (December, January and February) begins at the end of spring and lasts until the early autumn of the following year, the maximum anomaly occurring in February.

5. The SO has great effects on the characteristics of the circulation, center of the atmospheric activities, mean monthly zonal height and zonal wind velocity. However, the effect varies with season and latitude.

REFERENCES

Angell, J.k., (1981), Comparison of variation in atmospheric quantities with sea surface temperature variations in the equatorial eastern Pacific, *Mon. Wea. Rev.* Vol. 109, No. 2, 230–243.

Bi Muying, (1986), El Nino phenomena and 500 hPa atmospheric circulation in Northern Hemisphere, *Journal of Academy of Meteorological Science*, S.M.A., China, Vol. 1, No. 2, 175–184. (in Chinese with English abstract)

Bjerknes, J, (1969), Atmospheric teleconnections from the equatorial Pacific, *Mon. Wea. Rev.*, Vol. 97, No. 3, 163–172.

Chen Lieting, (1982), Interaction between the subtropical high over the north Pacific and sea surface temperature of the eastern equatorial Pacific, *Scientia Atmospherica Sinica* Vol. 6, No. 2, 148–156.

(in Chinese with English abstract)

Chen,W.Y.,(1982),Fluctuations in Northern Hemisphere 700 hPa height field associated with the Southern Oscillation. *Mon. Wea. Rev.*, Vol. 110, No. 7, 808–823.

Chen, W.Y., (1982), Assessment of Southern Oscillation sea level pressure indices, *Mon. Wea. Rev.*, Vol. 110, No. 7, 801–807.

van Loon, H & R.A. Maddgen, (1981), The Southern Oscillation Part I: Global association with pressure and temperature in northern winter, *Mon. Wea. Rev.*, Vol. 109, No. 6, 1150–1162.

van Loon & J.C. Rogers, (1981), The Southern Oscillation Part II: Associations with change in the middle troposphere in the northern winter, *Mon. Wea. Rev.*, Vol. 109, No. 6, 1163–1168.

van Loon, H. and C.C. Repapis, (1982), The Southern Oscillation in the atmosphere, *Mon. Wea. Rev.*, Vol. 110, No. 3, 225–229.

Mao Tiansong & Xu Naiyou, (1985), A preliminary study on El Nino phenomena and the influence of it on the summer monsoon circulation over East Asia, *Journal of Tropical Meteorology*, Vol. 1, No. 1, 19–26. (in Chinese with English abstract)

Pan Yihong & Oort A.H., (1983), Global climate variations connected with sea surface temperature anomalies in the eastern equatorial Pacific Ocean for 1958–1973 period, *Mon. Wea. Rev.*, Vol. 111, No. 7, 1244–1258.

Quinn, W.H., (1974), Monitoring and predicting El Nino invasions, *J. Appl. Meteor.*, Vol. 13, 825–830.

Trenberth, K.E., (1983), Signal versus noise in the Southern Oscillation, *Mon. Wea. Rev.*, Vol. 112, No. 2, 326–332.

Wang Shaowu, (1984), The Southern Oscillation/El Nino during 1982–1983, *Sci. & Tech. of Meteor.* No. 3, 1–7.

Wang Shaowu, (1985), The El Nino year during the 1860–1979 period, *Science Bulletin*, No. 1, 52–56.

Zang Hengfan and Wang Shaowu, (1984), The influence of sea surface temperature of equatorial east Pacific Ocean on the atmospheric circulation in low latitude, *Acta Oceanologica Sinica*, Vol. 6, No.1, 16–24. (in Chinese)